Article ID：1007−7294(2026)06−0957−13

Experimental Study of Mechanical Properties and Recovery Properties of Shape Memory Alloy Hybrid Composites under Static Bending

LI Xiao−bin [1,2,3], *ZHAO Zhe−ji* [1,2,3], *LI Meng−zhen* [1,2,3], *ZHANG Yi−heng* [1,2,3], *CHEN Wei* [1,2,3], *LI Chun−bao* [1,2,3]

(1. Ship Shock Damage and Safety Protection Key Discipline and Technology Research Center, Wuhan University of Technology, Wuhan 430063, China; 2. Ship Impact and Protection of Hubei Province Key Discipline Laboratory, Wuhan University of Technology, Wuhan 430063, China; 3. School of Naval Architecture, Ocean and Energy Power Engineering, Wuhan University of Technology, Wuhan 430063, China)

Abstract: To enhance the bending mechanical properties of fiber-reinforced plastics (FRP) and address rapid damage repair under multiple bending loads, an improved shape memory alloy hybrid composite (ISMAHC) was developed by embedding layered orthogonal shape memory alloy (SMA) wires into FRP. Three-point bending and water bath recovery tests were performed on traditional single-layer unidirectional SMA hybrid composites (SMAHC), ISMAHC and FRP. The effects of layered orthogonal SMA configuration on stiffness, strength, and recovery capability were compared and investigated. Results demonstrate that SMA wires form a coupling effect with FRP, increasing the bending modulus. Furthermore, ISMAHC has higher stiffness due to its orthogonal architecture. The water bath recovery tests indicate that SMAHC and ISMAHC possess good deflection recoverability and mechanical property recoverability after multiple bending loadings. The deflection recovery rate of the first bending test is greater than 60%, and that of the second bending test is greater than 30%. Additionally, the bending modulus and bending strength recover more than 30%, with ISMAHC showing superior recoverability.

Key words: shape memory alloy hybrid composites; recovery properties; mechanical properties; static bending

CLC number: U668.5 **Document code:** A **doi:** 10.3969/j.issn.1007−7294.2026.06.008

0 Introduction

Fiber-Reinforced Plastics (FRP) have high specific strength and excellent impact resistance[1], rendering them widely adopted in marine engineering, particularly for ship and offshore structural applications[2−4]. During marine service, FRP components in ship structures experience diverse loadings, with bending being the primary load-bearing mode[5]. Consequently, bending mechanical properties are critical for ensuring the structural integrity of marine FRP components[6−8]. It is worth noting that ship structures are subjected not only to single bending loads but also to multiple bending loads in practical service. Enhancing bending

Received date：2025−10−18

Foundation items：Supported by the National Natural Science Foundation of China (52571364)

Biography：LI Xiao-bin (1971−), male, Ph.D., professor, E-mail: lxbmark@163.com; LI Chun-bao (1988−), male, Ph.D., assistant professor, corresponding author, E-mail: leecubao@whut.edu.cn.

performance and developing rapid damage mitigation strategies for FRP under cyclic bending have emerged as critical challenges in marine engineering. To develop smart composites with high specific strength, high specific stiffness, and self-recovery capability, researchers have integrated shape memory alloys (SMA)—notably featuring superelasticity, shape memory effect, and high damping[9−12] —into FRP matrices, creating SMA hybrid composites (SMAHC). A series of studies has been conducted on the static mechanical properties[13−19] and recovery properties[20−26] of SMAHC.

Studies on the static mechanical properties of SMAHC focused on the mechanical properties of the material under tension and the post-flexural behavior of different structures. Shariat et al[13] investigated the deformation behavior of SMAHC under tensile loading and the shape recovery properties during the heating process. A constitutive equation was derived to describe the mechanical properties of SMAHC under tensile loading. Hui et al[14] conducted tensile tests with constrained recovery tests on SMAHC. A modified model based on Brinson's constitutive equation was further developed to effectively predict the relationship between structural recovery stress and temperature. Akbari et al[16] numerically investigated the buckling behavior of thin-walled composite shells embedded with SMA wires. It was found that the critical buckling load of the structure was increased by 35% due to the incorporation of SMA wires. Patil et al[18] investigated the static deformation and equivalent stresses of SMAHC at different temperatures. Rasid et al[19] explored and analyzed the post-buckling behavior of SMAHC and developed a post-buckling finite element model for SMA. It was found that the post-buckling path will be more stable with the addition of SMA wires to the composite plate.

In terms of the recovery properties of SMAHC, Dezaki et al[23] focused on combining SMA with fiber reinforcements to prepare dynamic hybrid composites, and tested their robustness and controllability. It was found that the surface deflection could be controlled by temperature regulation. Bollas et al[24] investigated the problem of high restoring force generated by single SMA wires in composites under confined conditions, and found that these wires act as an internal stress generator in SMAHC. However, the damage mechanisms and bending mechanical behavior of SMAHC remain underexplored, with particular gaps in understanding the post-recovery property evolution.

In this study, an ISMAHC was designed to improve the bending mechanical properties of fiber-reinforced plastics and their damage management ability under multiple bending loads. This paper investigated the damage characteristics, bending mechanical properties, and the variation of mechanical properties after heating recovery of SMAHC and ISMAHC under bending loads through three-point bending and water bath recovery tests. Both experimental tests and theoretical calculations were carried out to analyze the mechanical and recovery properties of SMAHC and ISMAHC under bending loads.

1 Structure design and preparation

Pinto et al[21] stated that the layered cross-shaped wires material can improve the structural stiffness of composite materials. Moreover, the positive hybridization effect with the composites modifies the energy dissipation mechanism of the structure and reduces the degree of intralaminar damage in the composite structure. Rim et al[20] demonstrated that composites with monolayer isotropic SMA wires exhibit partial deflection recovery under post-impact quasi-static loading. To address these limitations, this study engineers ISMAHC by strategically interleaving layered orthogonal SMA wires within glass fiber composites, targeting enhanced strength and thermomechanical recoverability. ISMAHC is composed of 12 layers of SW220 glass

fiber orthogonal nonwoven fabric with SMA wires embedded between the fourth and fifth layers and between the eighth and ninth layers of the structure. The SMA wires feature nickel-titanium (NiTi) filaments with a diameter of 0.3 mm and a transverse pitch of 5 mm. The schematic structure is shown in Fig.1(a).

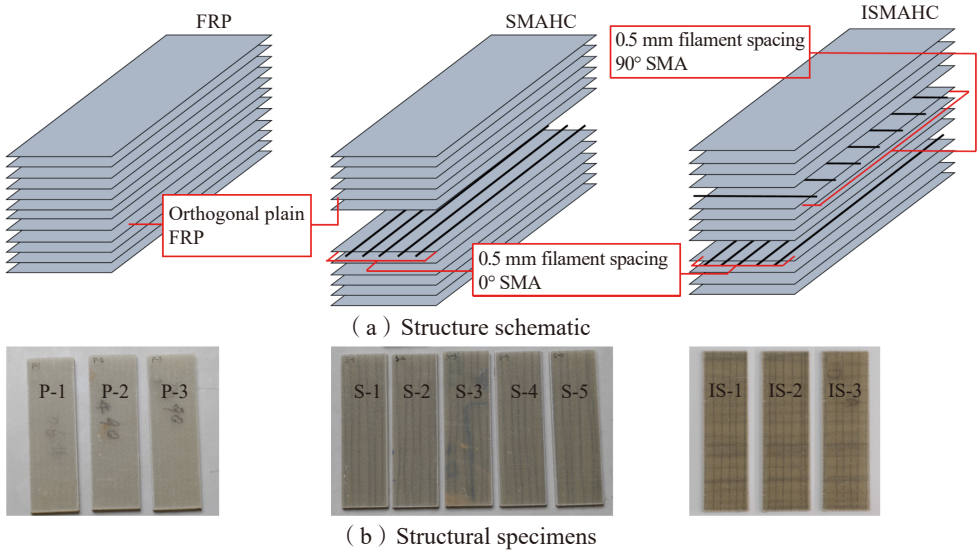


Fig.1 Schematic of the structures and the specimens of the test

To fabricate ISMAHC, SW220 high-strength fiberglass nonwoven is bonded by means of a vinyl resin adhesive. SW220 high-strength fiberglass nonwoven has a surface density of 240 g/m^2, a tensile modulus of elasticity of 86.4 GPa, a tensile strength of 4.6 GPa, and an elongation at break of 5.3%. SMA wire material with a diameter of 0.3 mm is selected. The composite structure is manufactured via the Vacuum Assisted Resin Injection molding (VARI) process. The DARDI's DWJ1425-FC waterjet cutting machine is employed to cut the initial composite material board by waterjet. For comparative tests, a conventional SMAHC embedded with a single layer of SMA wires in FRP as proposed in the literature [20,27−28] is fabricated using the same process. After waterjet cutting, test specimens with a length of 80 mm and a width of 25 mm are obtained. The FRP specimens are labeled as P-1, P-2, and P-3; the SMAHC specimens are labeled as S-1, S-2, S-3, S-4, and S-5; and the ISMAHC specimens are labeled as IS-1, IS-2, and IS-3. The specimens of the FRP, SMAHC, and ISMAHC are shown in Fig.1(b).

2 Design of the experiment

The first three-point bending test was performed on the specimens using an electronic universal testing machine in accordance with the ASTM D790 standard. After aligning the specimen with the punch of the universal material testing machine, the specimen was subjected to bending loads at a loading rate of 3 mm/min. In the loading protocol, a load cessation criterion was defined as 60% of the historical maximum force recorded by the universal testing machine during the test. This design ensured that specimens underwent a complete bending failure evolution while avoiding complete structural fracture, thus safeguarding experimental safety. During the test, a video camera was employed to record the bending damage process of the specimen. Following static three-point bending to failure, the specimen was heated to investigate its structural recoverability. To uniformly heat the specimens at a constant low temperature and to clearly observe their recovery behavior, the water-bath heating method was employed. The specimens were

heated in a 56 ℃ water bath with a DF-101 collector-type thermostatic heater; this temperature was set just above the end of the martensitic phase transition temperature of the SMA wires. This enables the SMA wires to generate recovery forces when the composite is not in a glassy state, thereby avoiding any impact on the strength of the composite. A video camera was adopted to record the response process and the vernier calipers were utilized to measure the deflection during the experiment. Subsequently, a second three-point bending test was then conducted to investigate the recovery of the structure's strength and stiffness. Finally, a second water bath recovery test was conducted to investigate the secondary recoverability of the structure. The flowchart of the series experiment is shown in Fig.2.

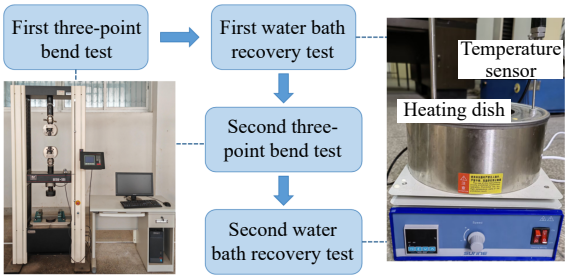


Fig.2 Flow chart of the series of experiments

3 Experimental results and analysis

3.1 Damage morphology

Fig.3 shows the damage morphology of FRP, SMAHC and ISMAHC after the first three-point bending test. Although all specimens exhibited similar damage patterns, the different arrangement of shape memory alloy wires resulted in differences in the spatial layout and strength of damage propagation.

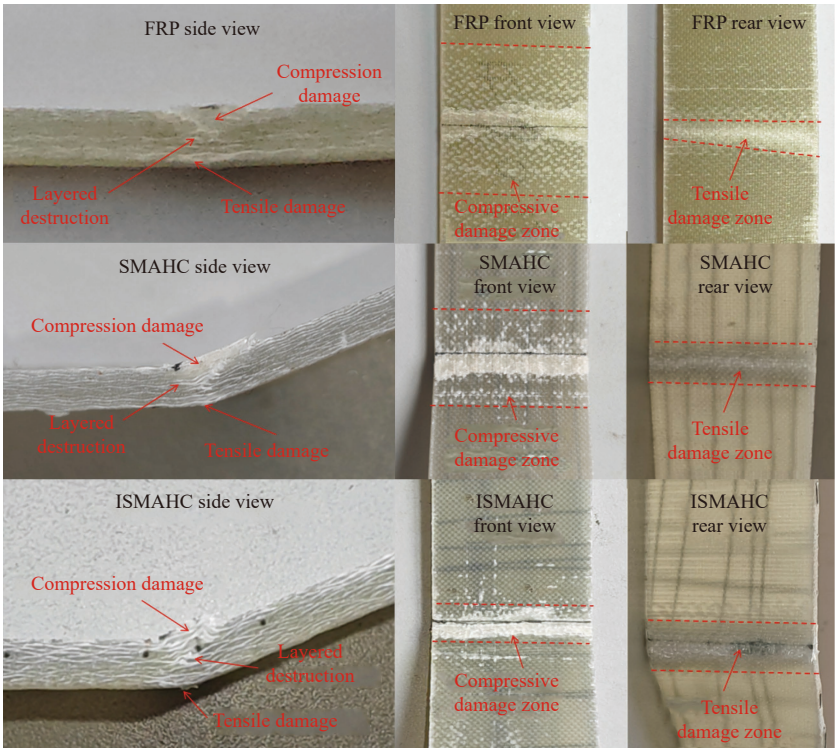


Fig.3 Damage morphology diagram of the specimen after the first three-point bending test

Compressive damage is observed on the upper surface of all specimens during bending. The degree of compressive damage is reduced by the addition of SMA wires. In conclusion, the compressive damage on the upper surface of the structure during bending is pronounced in the FRP specimens. Obvious matrix cracking and fiber breakage are clearly observed in the area directly beneath the indenter. Outside the direct range of

action of the indenter there is still visible damage with dense "white spots". Compared with the FRP structure, the compressive damage zone on the upper bending surface of the SMAHC is more concentrated, mainly focusing on the area directly under the indenter. For the ISMAHC, the compressive damage zone on its upper bending surface is even more concentrated. Outside the area directly under the indenter, there is almost no compressive damage in the structure. Furthermore, the edges of the compressive damage region of ISMAHC are closer to a straight line, which demonstrates that the damage is more uniform.

The tensile damage observed on the lower surface indicates that the embedded SMA wires promote a more pronounced evolution of tensile damage in the structure, which can be attributed to the load-transfer mechanism of SMA wires. It is observed that the tensile damage region on the lower surface of the FRP specimen is small and heterogeneous. The damage patterns are mainly the debonding of the fibers from the matrix material. The tensile damage of SMAHC is concentrated, with the shape of the damage being basically straight. SMAHC exhibits significant fiber breakage with the appearance of fiber break zones. ISMAHC demonstrates nearly double the tensile damage area, featuring dense fiber fractures and matrix microcracking.

The embedding of SMA wires increases the delamination damage region of the composite structure. This might be because the fact that the interleaving of SMA wires disrupts the interfacial properties of the structure. On the contact surface between the SMA wires and the FRP, micro-defects inevitably occur during the fabrication process due to the different material properties. These micro-defects can lead to delamination damage of the structure during bending.

Following the first water bath recovery, both SMAHC and ISMAHC specimens exhibited measurable deflection recovery, attributed to SMA wires actuation above martensitic finish temperature. Damage morphology analysis revealed unchanged matrix cracking patterns in SMAHC after recovery, despite deflection reduction. This is because the protruding parts of the cracks detached from the main structure, as shown in Fig.4. The compressive damage that occurs in the structure during the first three-point bending remains almost invariable after the recovery. Recovery heating induced fiber layer re-alignment (Fig.4), mitigating interlaminar delamination but not eliminating matrix cracks. The region of tensile damage developed during the first three-point bending did not change significantly after recovery, but the fiber breaks in its center are more conspicuous. The damaged fibers extend outside the main structure due to deflection recovery, causing the lower surface of the structure to appear rougher. ISMAHC had similar recovery behavior but less fiber protrusion (Fig.4), consistent with its narrower tensile damage zone.

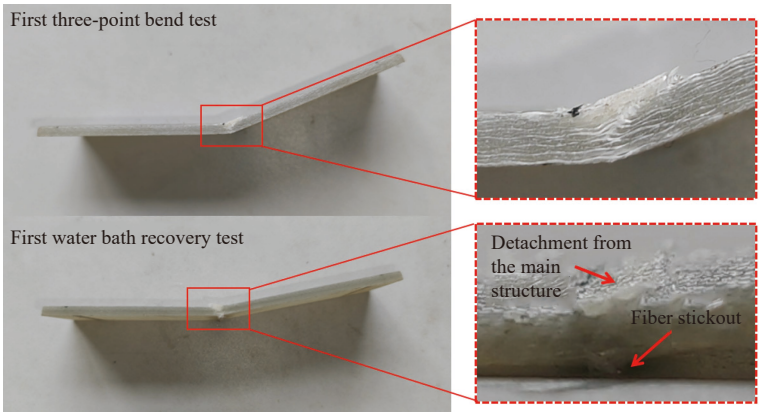


Fig.4 Variation of damage morphology of SMAHC samples after water bath recovery test

3.2 Stress-strain relationship

Load and deflection data from three-point bending tests were calculated using bending stress and strain formulas respectively. The bending stress-strain curves were obtained for each specimen.

Fig.5 illustrates the bending stress-strain curve of the FRP during the first three-point bending test. Linear elastic behavior dominates up to $\varepsilon = 0.015$, corresponding to the elastic deformation of fiberglass reinforcement. At this stage, the structure is primarily subjected to matrix compressive damage. Upper surface inspection identifies that fiber-matrix debonding zones ("white spots") extended bilaterally from the indenter contact line. At a strain of 0.022, the FRP reaches its ultimate strain, at which point matrix cracking occurs on the upper surface. Consequently, the load-bearing capacity of the structure is diminished. Post-ultimate behavior features two distinct plateau regions, revealing damage evolution mechanisms. The first plateau region is caused by the continued evolution of compressive damage on the upper surface of the structure. Damage propagates as wedging cracks through the laminate thickness, driven by compressive shear stress. This results in the formation of the first plateau region where the structural load-carrying capacity cannot increase. At a strain of 0.027, the structural compressive damage evolution is basically complete and the structural load-carrying capacity decreases. The structure is in the second plateau region after the ultimate strength at the strain range of 0.029 to 0.031. At this stage, the tensile damage of the structure continues to evolve in the thickness direction.

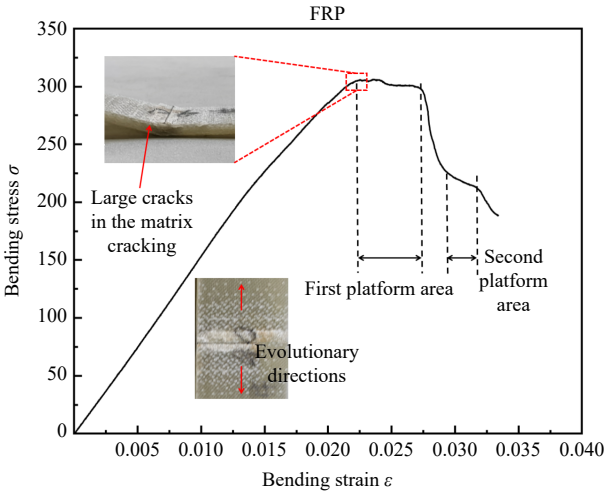


Fig.5 Bending stress-strain curve of the FRP in the first three-point bending test

The bending stress-strain curves of the SMAHC during the first three-point bending test are presented in Fig.6(a). During static bending, the stress-strain relationship of SMAHC is similar to that of FRP. However, compared with FRP, its first plateau region is shorter. This discrepancy may stem from the fact that SMAHC compressive failure being primarily localized near the contact surface, in contrast to the FRP evolutionary behavior observed in the first plateau region. The second plateau region of the structure mainly undergoes further evolution of tensile failure, which is longer compared to the evolution of FRP in this region. This may be due to the presence of SMA wires, which transfer the tensile force generated by bending in the structure to the composite material, resulting in a prolonged evolution of tensile failure and a more complete degree of evolution.

Fig.6(b) presents the bending stress-strain curve of the ISMAHC during the first three-point bending test. During static bending, the stress-strain relationship of ISMAHC is similar to that of SMAHC. The prolonged evolutionary time of the first plateau region in ISMAHC is primarily attributed to the occurrence of more severe matrix damage during flexural loading. Compared with the second plateau region of the SMAHC, the second plateau region of the ISMAHC is longer. This may be due to the effect of the transverse SMA wires, which leads to a more uniform evolution of the structure and a longer time for the evolution of tensile failure and a more complete degree of failure.

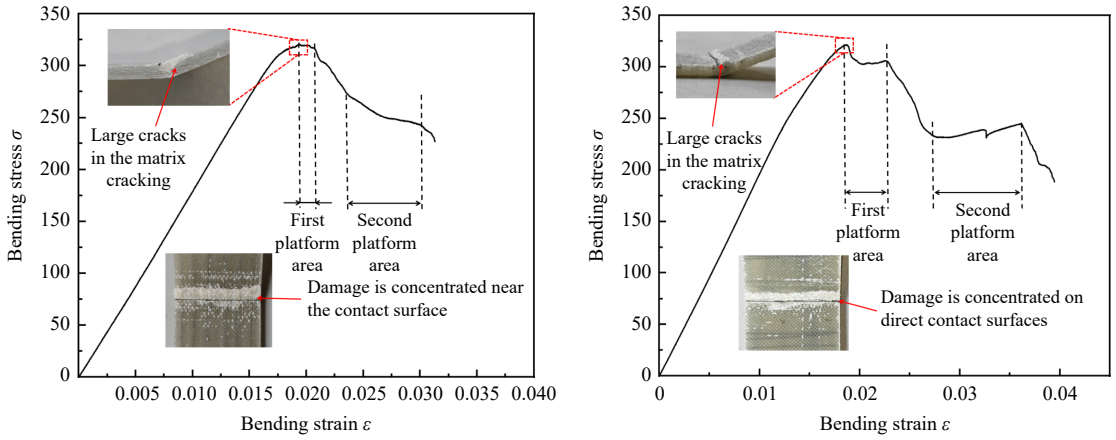


Fig.6 Bending stress-strain curve of the SMAHC and ISMAHC in the first three-point bending test

3.3 Response capacity

Since SMA has shape memory properties, shape memory metal reinforced composites can be made to have certain self-recovery effects under heating conditions through the shape memory effect of SMA after combining it with ordinary FRP materials[23−24]. This study aims to investigate whether the composite structure after adding SMA wires has self-recovery properties and how its self-recovery process evolves. We firstly studied the deformation of SMAHC and ISMAHC in a series of self-recovery tests, as shown in Fig.7, it is noteworthy that the incorporation of SMA wires endows the composite structures with a certain deflection recovery ability after bending damage occurs. Among the tests, the self-recovery effects of the structures after heating in the water bath are rapid, with all completing the self-recovery process within 5 s. These results validate rapid bending recovery as a key attribute of SMAHC/ISMAHC, enabled by SMA's thermomechanical actuation.

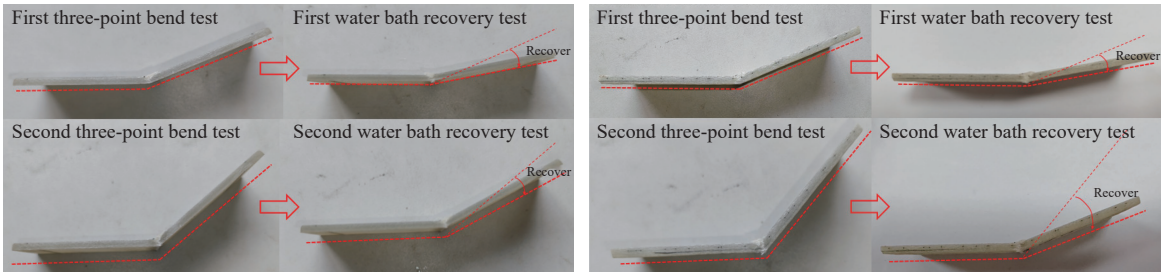


Fig.7 Deformation of SMAHC and ISMAHC during recovery test

Following data acquisition of peak deflections in the self-recovery test series, deflection recovery ratios were calculated and plotted as a bar graph (see Fig.8). The first water bath heating deflection recovery was found to be high for both SMAHC and ISMAHC structures, with an average deflection recovery of 67.60% for SMAHC and 80.41% for ISMAHC. This indicates that additional SMA wires are able to considerably restore the deflection of the structure. The average deflection recovery of ISMAHC is 12.81% higher than that of SMAHC, which has a better first deflection self-recovery effect. This is likely due to a layered cross of SMA wires allows the restoring force to be applied more evenly through the wires throughout the bent sheet. Therefore, it has stronger flexural self-recovery ability.

The bending deformation of the specimens in the second test was larger than that in the first one. Nevertheless, the composite structure still had the ability to self-recover after the second three-point bending

test, and still had a larger deflection recovery. Recovery kinetics slowed in the second recovery, attributed to accumulated damage. This may be due to the fact that the delamination damage occurring after the second three-point bending is more extensive, resulting in delamination and debonding between the SMA wires and the high-strength fiberglass scrim. This made it difficult for the restoring force provided by the SMA phase transition to act well enough to restore deflection to the composite structure. During the water bath heating self-recovery, the recovery rate of ISMAHC was higher than that of SMAHC. This phenomenon could be ascribed to the transmission of the recovery force by the transverse SMA wires. It is found that both SMAHC and ISMAHC have the ability to recover deflection twice, but the second deflection recovery of both is less than the first recovery. The average deflection recovery of SMAHC is 30.68%, which is 36.92% less than the first recovery. However, the average deflection recovery of ISMAHC is 57.52%, which is 22.89% less than the first recovery. This indicates that the ISMAHC has better deflection recovery for secondary bending damage and retains a stronger self-recovery capability in the case of multiple bending damage.

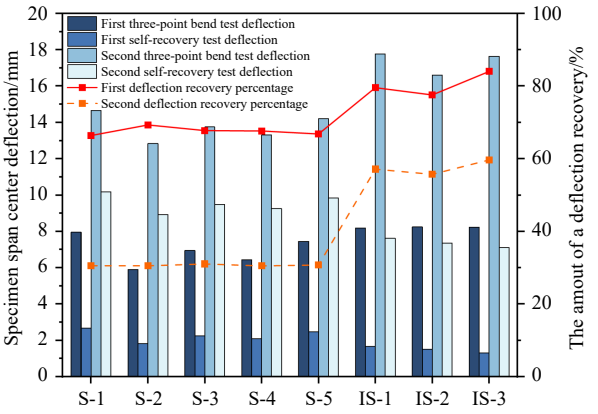


Fig.8 Bar chart of deflection recovery data of test specimens

4 Discussion

4.1 Effect of SMA wires on the mechanical properties of structures

Based on the analysis of the stress-strain curves of FRP, SMAHC and ISMAHC obtained from the experiments, it is worth noting that the bending modulus of SMAHC and ISMAHC are higher than those of FRP. The bending modulus of SMAHC is 20.11% higher than that of FRP, and the bending modulus of ISMAHC is 27.20% higher than that of FRP. To investigate the principle of SMA wires in composite structures to significantly increase the bending modulus of the structure, SMAHC was used as an example to analyze and calculate its composite structure.

Firstly, the boundary conditions of the experiment are analyzed. Since the fixture does not fully restrict the longitudinal displacement of the composite structure during the test, the force on the SMA filament during three-point bending of the structure is modeled as a simply supported beam based on the flat section assumption. According to the bending theory of simply supported beams[29] the relationship between the deflection in the middle of the beam $\omega_{\max}$ and the magnitude of the concentrated force acting in the middle of the simply supported beam can be obtained by the following equation

$$\omega_{\max} = \frac{Fl^3}{48EI} \tag{1}$$

where, F is the mid-span force, l is the span length of the specimen, E is the elastic modulus, and I is the moment of inertia. The magnitude of the concentrated load applied at the midspan of a simply supported beam equals that of the reaction force exerted by the beam on the loading member as a result of the equilibrium principle in statics. By combining the Eq.(1) and the inertia moment formula of the cylinder, we obtained the relationship between the reaction force acting on the SMA filament in bending (F_{SMA}) and the maximum deflection in the span of the SMA filament can be obtained as

$$F_{\mathrm{SMA}}=\frac{3\pi Ed^4}{4l^3}\omega_{\max} \tag{2}$$

To obtain the modulus of elasticity of the SMA filament, the SMA filament was loaded using an Instron 5882 electronic universal material testing machine with equal strain rate control. To be able to remove the effect of strain rate on the stress-strain relationship of SMA, quasi-static stretching of SMA was performed with a strain rate of 1 mm/min. After obtaining the experimental data, linear data fitting was performed on the martensitic phase of SMA material in the linear elastic stage using the principle of least squares. The slope of the obtained function is the martensitic elastic modulus E_S of the material. The elastic modulus in Experiment 1 was 9.638 GPa, and the elastic modulus in Experiment 2 was 9.490 GPa (see Fig.9). The average of the two values was taken as 9.564 GPa as the martensitic elastic modulus of the material.

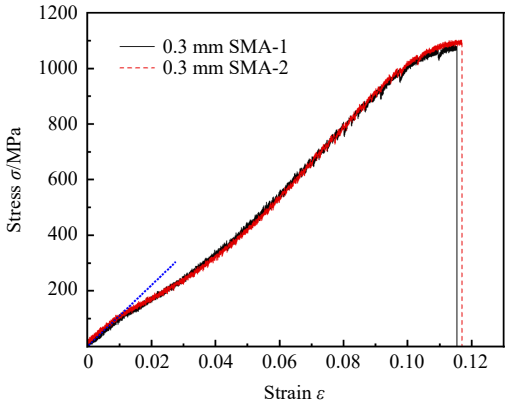


Fig.9 SMA wires elastic modulus testing data

In the experiment, each SMAHC specimen was interleaved with 6 SMA wires. The theoretical calculation of the force provided by the SMA wires during structural bending and the maximum deflection of the wire span were converted into the bending stress and bending strain of the composite structure using the calculation formula of bending stress and bending strain. Thus, the increase in strength of the composite structure during the bending process of the composite structure due to the addition of SMA wires in theoretical calculations can be obtained. When comparing the theoretical results with experimental data, the stress at a strain of 0.01 under elastic conditions was selected as the reference point (see Fig.10). Theoretical calculations incorporating SMA wires predicted a strength enhancement of 0.004 25 MPa in the composite structure during bending. This predicted increase was significantly smaller than the 24.8 MPa improvement observed experimentally. This indicates that the addition of SMA wire material enhances the bending modulus of the structure, through a coupling effect, rather than a simple additive effect.

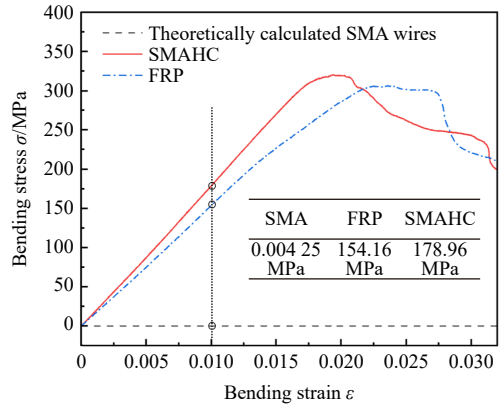


Fig.10 Comparison of theoretical calculation intensity increase and experimental data

From the morphology of the experimental results, it is clear that after adding SMA wires to the structure, the tensile failure area of the lower surface of SMAHC significantly increases compared with that of FRP, and the degree of damage is more severe. It can be found that the interaction between SMA wires and glass fiber reinforced composite material leads to a more complete evolution of tensile failure of the overall structure under bending load, thereby achieving higher bending modulus of SMAHC in bending failure.

4.2 Effect of SMA wires on structural recovery capacity

The addition of SMA wires enables the SMAHC to recover deflection after bending failure. To investigate the recovery of mechanical properties of SMAHC in addition to deflection recovery at the

macroscopic scale, and to explore the principles of structural recovery ability and secondary bending resistance, further processing and analysis of experimental data were conducted.

The maximum value of the two stress-strain curves of SMAHC and ISMAHC is taken as the bending strength σ_{max} of the structure. The slope of the initial linear segment on the load deflection curve is processed to obtain the bending modulus of the structure. The bending modulus and bending strength of specimens with different structures are presented in Fig.11. It was found that both the bending strength and bending modulus of the structure recovered to a certain extent after being heated in a water bath. Among them, the bending modulus of the SMAHC recovered by 30.85%, and the bending strength recovered by 30.78%. The bending modulus of ISMAHC has recovered by 30.83%, and the bending strength has recovered by 37.78%. The recovery of the bending modulus and bending strength of the structure may be owing to the fact that during the three-point bending test load application, the SMA wires along the length direction of the specimen transfer force to the high-strength glass fiber layer, mainly transmitting axial tensile load. The composite structure continues to bear tensile load outside the already damaged area, and the tensile failure area of the structure continues to expand. The degree of damage in the damaged area continues to increase. The greater bending strength recovery of the ISMAHC may be attributed to the more uniform distribution of the recovery force generated by the transverse wires during heating.

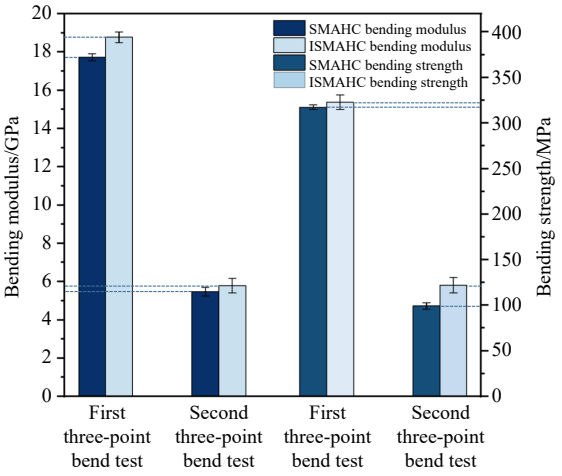


Fig.11 Multiple bending modulus and bending strength data of SMAHC and ISMAHC

From the stress-strain relationship obtained from the experiments (Fig. 12), it is concluded that ISMAHC has a more durable load-bearing capacity during secondary bending failure due to the interleaving of transverse SMA wires. Its second bending strength is 24.83% higher than that of SMAHC. Comparing the second three-point bending failure morphology of SMAHC and ISMAHC (Fig.13), it is concluded that the fiber tensile failure on the lower surface of ISMAHC evolves more fully to both sides, and the outermost fiber has already experienced fracture, and thus there is less evolution to both sides. The closer the composite layer embedded with SMA wire is to both sides, the more complete the tensile evolution to both sides. This may be owing to the transmission of tensile force and the enhancement of material strength by the SMA wires. Compared to SMAHC, the ISMAHC has transverse SMA wires that can cause cracks in the structural matrix to redirect during evolution due to compression failure. The cracks alternate between continuing to develop toward the center of the structure and developing laterally between the layers. This

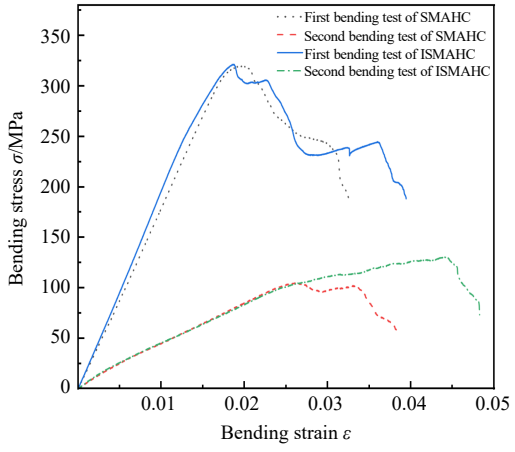


Fig.12 The stress-strain relationship of SMAHC and ISMAHC

restricts the damage zone of compressive damage to prevent cracks from propagating directly to fracture, which would induce the structure to completely lose its flexural load-bearing capacity.

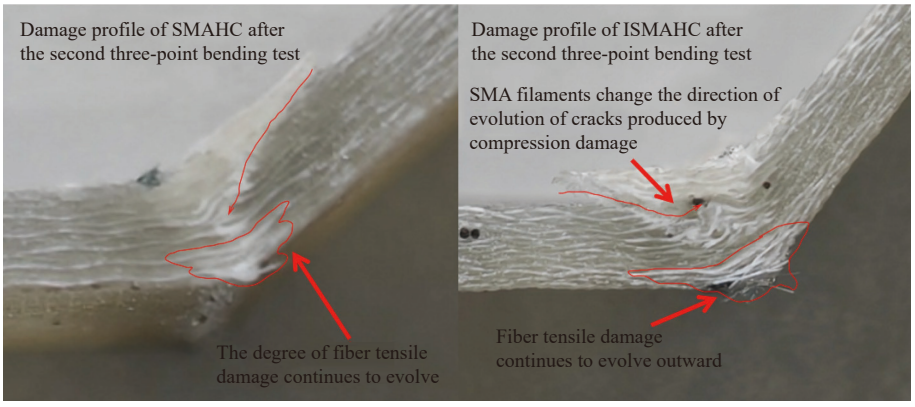


Fig.13 Comparison of local failure morphology of SMAHC and ISMAHC in the second three-point bending

5 Conclusions

This article aims to investigate the failure characteristics, flexural mechanical properties and variations in mechanical properties after recovery of SMAHC and ISMAHC under bending loads through three-point bending tests and water bath recovery tests. The main conclusions obtained are as follows:

(1) The addition of SMA wires reduces the compressive failure area of the structure, increases the delamination and tensile failure areas, and yields a more uniform damage evolution. Due to the supporting and transferring effect of tensile force by SMA wires, a longer second plateau region appears in the structure. In ISMAHC, the lateral force transmission of SMA wires results in more uniform failure and extended second plateau evolution time compared to SMAHC. During multiple three-point bending, the compressive failure area remains stable, while tensile failure evolves significantly along both the longitudinal and thickness directions of the structure.

(2) SMA wires can increase the bending modulus of FRP. Theoretical and experimental results reveal that the interaction between SMA wire and glass fiber reinforces composite material, which leads to a more complete evolution of tensile failure of the overall structure under bending load. This mechanism ultimately enhances the bending modulus of SMAHC during bending failure.

(3) The ISMAHC demonstrates better multiple deflection recoverability. The SMAHC and ISMAHC also have the ability to recover mechanical properties, with their bending modulus and bending strength recovering by over 30%. This improvement stems from SMA wires transferring axial tensile loads to high-strength glass fibers during bending, ultimately leading to an expansion of the tensile failure area of the structure.

References

[1] Rajak D K, Pagar D D, Kumar R, et al. Recent progress of reinforcement materials: A comprehensive overview of composite materials[J]. Journal of Materials Research and Technology, 2019, 8(6): 6354–6374.

[2] Bhong M, Khan T K H, Devade K, et al. Review of composite materials and applications[J]. Materials Today: Proceedings, 2023.

[3] Ahmed O S, Aabid A, Mohamed Ali J S, et al. Progresses and challenges of composite laminates in thin-walled structures: A systematic review[J]. ACS omega, 2023, 8(34): 30824–30837.

[4] Crupi V, Epasto G, Napolitano F, et al. Green Composites for Maritime Engineering: A Review[J]. Journal of Marine Science and Engineering, 2023, 11(3): 599.

[5] Wu J, Zhang X M, Hu M Y, et al. Bending stress of composite hull cap type reinforced plate[J]. Journal of Ship Mechanics, 2023, 27(7): 1084–1095.

[6] Shen Y L, Li Y G, Huang X H, et al. Experimental study on cumulative characteristics of repeated impact damage in composite sandwich panels[J]. Journal of Ship Mechanics, 2023, 27 (10): 1542−1549.

[7] Guo J, Pan B B, Cui W C, et al. A review of research on deep-sea actuators and biomimetic robots based on intelligent materials [J] Journal of Ship Mechanics, 2022, 26(2): 301−313.

[8] Wu J, Wang W B, Zhang T T, et al. Strength prediction of glass fiber epoxy resin composite laminates under moderate strain rate[J]. Journal of Ship Mechanics, 2021, 25(9): 1222−1231.

[9] Baitab D M, Majid D L, Abdullah E J, et al. Flutter performance of shape memory alloy-embedded 3D woven flexible composite plate under subsonic flow[J]. Journal of Industrial Textiles, 2022, 51(3_suppl): 4290S–4328S.

[10] Angioni S L, Meo M, Foreman A. Impact damage resistance and damage suppression properties of shape memory alloys in hybrid composites—A review[J]. Smart Materials and Structures, 2010, 20(1): 013001.

[11] Shukla U, Garg K. Journey of smart material from composite to shape memory alloy (SMA), characterization and their applications-A review[J]. Smart Materials in Medicine, 2023, 4: 227–242.

[12] De Rosa I M, Sarasini F, Sarto M S, et al. EMC impact of advanced carbon fiber/carbon nanotube reinforced composites for next-generation aerospace applications[J]. IEEE Transactions on Electromagnetic Compatibility, 2008, 50(3): 556–563.

[13] Shariat B S, Liu Y, Meng Q, et al. Analytical modelling of functionally graded NiTi shape memory alloy plates under tensile loading and recovery of deformation upon heating[J]. Acta Materialia, 2013, 61(9): 3411–3421.

[14] Hui Y X, Xue Y J, Wang W W, et al. Experimental study on mechanical properties and recoverability of FRP/shape memory alloy composite materials[J]. Journal of Composite Materials, 2023, 40(9): 5302−5314.

[15] Hassanli S, Samali B. Buckling analysis of laminated composite curved panels reinforced with linear and non-linear distribution of Shape Memory Alloys[J]. Thin-Walled Structures, 2016, 106: 9–17.

[16] Akbari T, Khalili S M R. Numerical simulation of buckling behavior of thin walled composite shells with embedded shape memory alloy wires[J]. Thin-Walled Structures, 2019, 143: 106193.

[17] Khor W, Ravindran A R, Ciampa F, et al. Improving the damage tolerance of composite T-joints using shape memory alloy tufts[J]. Composites Part A: Applied Science and Manufacturing, 2023, 168: 107474.

[18] Patil R A, Rane S B, Kumbhar S B. Static analysis of shape memory alloy (SMA) reinforced composite[J]. Materials Today: Proceedings, 2022, 62: 6832–6836.

[19] Rasid Z A, Zahari R, Amran A, et al. Thermal post-buckling improvements of laminated composite plates using the active strain energy tuning approach[J]. Advanced Materials Research, 2011, 311: 2235–2238.

[20] Rim M S, Kim E H, Lee I, et al. Low-velocity impact characteristics of composite plates with shape memory alloy wires[J]. Journal of Theoretical and Applied Mechanics, 2011, 49(3): 841–857.

[21] Pinto F, Meo M. Mechanical response of shape memory alloy–based hybrid composite subjected to low-velocity impacts[J]. Journal of Composite Materials, 2015, 49(22): 2713–2722.

[22] Kim E H, Lee I, Roh J H, et al. Effects of shape memory alloys on low velocity impact characteristics of composite plate[J]. Composite Structures, 2011, 93(11): 2903–2909.

[23] Dezaki M L, Bodaghi M, Serjouei A, et al. Adaptive reversible composite-based shape memory alloy soft actuators[J]. Sensors and Actuators A: Physical, 2022, 345: 113779.

[24] Bollas D, Pappas P, Parthenios J, et al. Stress generation by shape memory alloy wires embedded in polymer composites[J]. Acta Materialia, 2007, 55(16): 5489–5499.

[25] Basit A, L'hostis G, Durand B. The recovery properties under load of a shape memory polymer composite material[J]. Materialwissenschaft und Werkstofftechnik, 2019, 50(12): 1555–1559.

[26] Burton D S, Gao X, Brinson L C. Finite element simulation of a self-healing shape memory alloy composite[J]. Mechanics

of Materials, 2006, 38(5−6): 525–537.

[27] Donadon M V, De Faria A R. Aeroelastic behavior of composite laminated shells with embedded SMA wires under supersonic flow[J]. Aerospace Science and Technology, 2016, 52: 157–166.

[28] Samadpour M, Asadi H, Wang Q. Nonlinear aero-thermal flutter postponement of supersonic laminated composite beams with shape memory alloys[J]. European Journal of Mechanics-A/Solids, 2016, 57: 18–28.

[29] Roylance D. Statics of bending: Shear and bending moment diagrams[EB/OL]. Cambridge, MA: MIT OpenCourseWare, 2000.

形状记忆金属复合材料在静力弯曲下的力学及回复特性试验研究

李晓彬[1,2,3], 赵哲稷[1,2,3], 黎梦真[1,2,3], 张以恒[1,2,3], 陈　威[1,2,3], 李春宝[1,2,3]

（1. 武汉理工大学 船舶冲击损伤与安全防护重点学科与技术研究中心, 武汉 430063; 2. 武汉理工大学 船舶冲击与防护湖北省重点学科实验室, 武汉 430063; 3. 武汉理工大学 船海与能源动力工程学院, 武汉 430063）

摘要: 为了提高纤维增强材料（fiber-reinforced plastics, FRP）的弯曲力学性能, 并解决多重弯曲载荷下的快速损管问题, 通过在纤维增强材料中嵌入分层正交形状记忆合金丝（shape memory alloy, SMA）, 得到了一种改进的形状记忆合金混合复合材料（improved shape memory alloy hybrid composite, ISMAHC）。对 FRP、嵌入单层 SMA 线的形状记忆合金混合复合材料和 ISMAHC 进行了一系列三点弯曲和水浴恢复试验。实验测试和理论计算证明 SMA 能与 FRP 结合产生耦合效应, 从而提高结构的弯曲模量。水浴恢复试验表明, SMAHC 和 ISMAHC 在多次弯曲加载后仍具有良好的挠度恢复能力和力学性能恢复能力。第一次弯曲试验的挠度恢复大于 60%, 第二次弯曲试验的挠度恢复大于 30%。弯曲模量和弯曲强度的恢复率均超过 30%, 其中 ISMAHC 的恢复能力更强。

关键词: 形状记忆金属复合材料; 回复特性; 力学特性; 三点弯曲

中图分类号: U668.5　　**文献标识码:** A

基金项目: 国家自然科学基金资助项目（52571364）

作者简介: 李晓彬（1971−）, 男, 博士, 教授, E-mail: lxbmark@163.com;

赵哲稷（2001−）, 男, 硕士;

黎梦真（1994−）, 男, 博士, 副教授;

张以恒（1992−）, 男, 博士, 副教授;

陈　威（1988−）, 男, 博士, 教授;

李春宝（1988−）, 男, 博士, 讲师, 通信作者, E-mail: leecubao@whut.edu.cn。